Hyperacute Changes in Glucose Metabolism of Brain Tumors After Stereotactic Radiosurgery: A PET Study

Ichiro Maruyama, Norihiro Sadato, Atsuo Waki, Tatsuro Tsuchida, Masanori Yoshida, Yasuhisa Fujibayashi, Yasushi Ishii, Toshihiko Kubota and Yoshiharu Yonekura

Departments of Radiology and Neurosurgery and Biomedical Imaging Research Center, Fukui Medical University, Fukui, Japan

Cultured tumor cells show a marked increase in deoxyglucose uptake as early as 3 h after single high-dose irradiation, reflecting hyperacute response of the cells to noxious intervention. To evaluate the hyperacute effect of high-dose irradiation on tumor glucose metabolism in vivo, we measured 2-[^{18}F]fluoro-2-deoxy-D-glucose (FDG) tumor uptake before and immediately after stereotactic radiosurgery. **Methods:** A total of 19 brain tumors (17 metastatic and 2 primary, a meningioma and a central neurocytoma) in eight patients were treated with stereotactic radiosurgery. The received dose was between 24 and 32 Gy delivered to the central target point in the tumor. FDG PET was performed within 1 wk before radiosurgery and again 4 h after treatment. The net influx constant (Ki) was calculated on a pixel-by-pixel basis using graphical analysis, and the Ki ratio of tumor to ipsilateral cerebellum was used as an index of FDG uptake of the tumor. **Results:** Eighteen of 19 irradiated tumors, all metastatic tumors and the meningioma, showed a 29.7% ± 14.0% increase in the Ki ratio, which was significantly higher than that of nonirradiated tumors (4.1% ± 3.6%, n = 8, $P < 0.0001$, analysis of variance). In metastatic tumors, an increase in the Ki ratio was significantly correlated with a decrease in the size of the irradiated tumors, as revealed by follow-up with CT or MRI ($r = 0.61$, $P = 0.012$, simple regression). The meningioma did not show a significant decrease in size, probably due to the short follow-up period. The central neurocytoma did not show any change in the Ki ratio or in tumor size. **Conclusion:** Serial FDG PET could be a potential tool for predicting the outcome of radiosurgery for brain tumors by detecting hyperacute changes in tumor glucose metabolism.

Key Words: PET; 2-[^{18}F]fluoro-2-deoxy-D-glucose; stereotactic radiosurgery; tumor glucose metabolism

J Nucl Med 1999; 40:1085–1090

Because of the high glucose use of many neoplasms (*1,2*), 2-[^{18}F]fluoro-2-deoxy-D-glucose (FDG) and PET are of demonstrated clinical value in detecting malignant tissue and quantifying changes in tumor glycolysis during and after treatment (*3,4*). After facilitated diffusion from plasma to tissue, FDG is phosphorylated by hexokinase and trapped intracellularly as FDG-6-PO_4. About 40 min after intravenous injection of FDG, the majority of the ^{18}F signal originates from intracellular FDG-6-PO_4. With a slow rate of dephosphorylation, FDG-6-PO_4 accumulates at a rate proportional to glycolysis (*3*).

Although several studies have stressed the usefulness of FDG PET for detecting therapeutic efficacy, which is reflected by a decline in FDG uptake (*5–7*), the onset of metabolic changes that reflect treatment effects rarely has been reported. Hautzel and Muller-Garter (*8*) found that tumor glucose uptake was enhanced after the application of 6 Gy (2 Gy/d) but constantly declined as the dose was increased. Furuta et al. (*9*) studied early changes in the glucose metabolism of human tumor xenografts. Only the most radiosensitive tumor showed an increase in FDG uptake 2 h after irradiation compared with a nonirradiated group. Rozental et al. (*10*) reported that glucose uptake ratios increased 25%–42% 1 d after radiotherapy and then decreased to between 10% above and 12% below the baseline 7 d after radiotherapy. Using cultured tumor cells, Fujibayashi et al. (*11*) observed a significant increase in glucose metabolism as early as 3 h after single high-dose irradiation, without any morphological change or change in cell number. Various oncogenes overexpressed in tumor cells respond rapidly to ionizing radiation (*12*). Increased expression of various growth-related genes also has been reported (*12,13*). Oncogene expression of these messenger ribonucleic acids increases within 10–30 min after irradiation but subsequently returns to baseline in 1 or 2 d (*12*).

To evaluate the hyperacute effect of high-dose irradiation in a single fraction on tumor glucose metabolism, we performed FDG PET before and immediately after radiosurgery.

MATERIALS AND METHODS

Patients

Eight patients (three men, five women; mean age 61.1 ± 18.7 y with brain neoplasms were included in this study (Table 1). Two patients each had a single, residual, primary brain tumor after

Received Jul. 17, 1998; accepted Aug. 25, 1998.

For correspondence or reprints contact: Norihiro Sadato, MD, PhD, Biomedical Imaging Research Center, Fukui Medical University, 23 Shimoaizuki, Matsuoka-cho, Yoshida-gun, Fukui, 910-11 Japan.

TABLE 1
Patient Characteristics and Radiation Doses in Radiosurgery

Patient no.	Age (y)	Sex	Origin/ histology	No. of lesions	Prior treatment	Dose (Gy)
Metastatic						
1	83	M	Lung	Multiple	None	25.6 25.6
2	55	M	Lung	Multiple	Surgery + WB 30 Gy	32.0 32.0 32.0* 24.0*
3	49	F	Lung	Multiple	None	32.0 32.0
4	80	F	Lung	Multiple	Surgery	32.0 32.0 32.0 24.0* 24.0*
5	61	M	Melanoma	Multiple	WB 30 Gy	32.0 32.0 24.0* 24.0* 32.0*
6	60	F	Colon	Single	None	32.0
Primary						
7	75	F	Meningioma	Single	Surgery	24.0
8	26	F	Central neuro-cytoma	Single	Surgery	24.0

*Dose of second radiosurgery.
WB = whole-brain radiotherapy.

partial resection. Six patients had metastatic brain tumors from the lung (n = 4), skin (melanoma) (n = 1) and colon (n = 1). Contrast-enhanced MR and CT images showed that five of these patients had multiple brain lesions and one patient had a single lesion. Two patients with metastases had undergone whole-brain irradiation (one of these patients also had the tumor resected), one patient had tumor resection only and three other patients never had been treated for the brain lesions before the present radiosurgery. In accordance with the criteria for radiosurgery in our hospital, none of the patients had active extracranial disease, and all were expected to survive at least 6 mo after treatment. None of the patients received chemotherapy during the study. Three patients received radiosurgery twice. The study protocol was approved by the Ethical Committee of Fukui Medical University, and all patients gave their written informed consent.

Stereotactic Radiosurgery

All patients were treated with 10-MV photons using a linear accelerator with a multiple-arc non-coplanar method in which irradiation accuracy was estimated to be within ±1 mm (*14,15*). The mechanical details of stereotactic radiosurgery have been described previously (*16*). With the patient under local anesthesia (xylocaine) and intravenous analgesics (pentazocine), Leksell's stereotactic frame was applied to the patient's head and fixed to the treatment bed. Axial CT was performed after the administration of a contrast agent to obtain sequential slices that were 1 mm thick at the target point and 5 mm thick through the entire head. Treatment planning software (Marui Medical Inc., Tokyo, Japan) was used to select the center of the tumor and to calculate the number of treatment arcs, start and stop angles for the linear accelerator gantry and couch angles. The 50% isodose line covered the periphery of the tumor, which was delineated by contrast-enhanced CT. All treatment procedures took about 2 h. With multiple metastases, another hour was required to treat each additional tumor. We irradiated no more than 3 tumors at a time, and the others were treated on a second occasion. Stereotactic radiosurgery was delivered with a sharp, peripheral dose falloff, resulting in minimal exposure of surrounding tissue (Fig. 1). The received dose ranged from 24 to 32 Gy, delivered to the central target point in the tumor (Table 1).

PET

Patients underwent a set of two consecutive FDG PET scans combined with each radiosurgery session. The first scan was obtained within 1 wk before radiosurgery, and the second scan was obtained 4 h after the session. Five patients underwent single radiosurgery, with a set of FDG PET scans. Three patients received radiosurgery twice (patients 2, 4 and 5 in Table 1). Patients 2 and 5 underwent two sets of FDG PET scans. In patient 5, the pretreatment FDG PET for the second radiosurgery was performed 2 wk after the first post-treatment FDG PET. Patient 4 underwent the first radiosurgery with a set of FDG PET scans. Without combined FDG PET, patient 4 received the second radiosurgery. Thus, 10 sets of FDG PET were performed, combined with radiosurgery, for a total of 20 scans.

FDG was produced by the method of Hamacher et al. (*17*) with an automated FDG synthesis system (NKK, Tokyo, Japan) and a small cyclotron (OSCAR3; Oxford Instruments, Oxford, UK). PET was performed with a General Electric Advance system (General Electric, Milwaukee, WI). The physical characteristics of this

FIGURE 1. Typical dose distribution superimposed on transaxial CT image. Tumor is included in area bounded by 80% isodose line (red), surrounded by narrow zone of rapid falloff in dose (blue; limited by 50% and 80% isodose lines).

scanner have been described in detail by DeGrado et al. (*18*). This system permits the simultaneous acquisition of 35 transverse slices with interslice spacing of 4.25 mm with septa (two-dimensional mode). Images were reconstructed to a full width at half maximum of 4.2 mm in both transaxial and axial directions. The field of view (FOV) and the pixel size of the reconstructed images were 256 and 2 mm, respectively. Transmission scans were obtained for 10 min using a standard pin source of $^{68}Ge/^{68}Ga$ for attenuation correction of the emission images. A dose of FDG (244–488 MBq) was administered for 10 s by means of the cubital vein. Dynamic scans were obtained up to 60 min after the injection, with arterial sampling. The mode of dynamic data acquisition consisted of four 30-s frames, eight 60-s frames and five 600-s frames. Plasma glucose concentrations were measured in all patients. From the time of the injection, 2 mL of arterial blood were sampled every 15 s in the first 2 min and then at 3, 5, 7, 10, 15, 20, 30, 45 and 60 min after the injection. The plasma radioactivity was measured by a scintillation counter, against which the PET camera was cross-calibrated, using a cylindrical phantom filled with the ^{18}F solution.

CT and MRI

CT and MRI were performed in all patients. A standard commercial CT system (High Speed Advantage RP scanner; General Electric-Yokogawa Medical System, Tokyo, Japan) was used to obtain contiguous transaxial images (FOV 23 × 23 cm, matrix size 512 × 512), with peak voltage of 120 kV and tube current of 250 mA, covering the entire brain in 7-mm slices and with 7-mm collimation. For contrast enhancement studies, 100 mL iopamidol, 300 mg/mL (Iopamilon 300; Nihon Schering, Osaka, Japan), or 100 mL iohexol, 300 mg/mL (Omnipaque 300; Daiichi Seiyaku, Tokyo, Japan), were injected intravenously as a bolus.

A 1.5-T MRI system (Signa Horizon; General Electric) was used to obtain transaxial T1-weighted fast spinecho images (repetition time [ms]/echo time [ms]/number of excitations = 333/10/3) and T2-weighted fast spinecho images (3500/88/2) (FOV 22 × 16 cm, matrix size 256 × 224), as well as sagittal and coronal T1-weighted images (FOV 22 × 22 cm, matrix size 256 × 224). Slice thickness was 5 mm. For contrast enhancement studies, 0.1 mmol/kg body weight of gadolinium-diethylenetriamine pentaacetic acid (Magnevist; Nihon Schering) was injected intravenously.

Data Analysis

The MRI and FDG PET datasets were transferred to a SUN workstation (SPARCstation MP20; SUN Microsystems, Mountain View, CA), and the MRI dataset was converted into a 256 × 256 matrix. The final voxel sizes of the MR and FDG PET images were 0.86 × 0.86 × 4 mm and 2 × 2 × 4.25 mm, respectively. Co-registration of FDG PET and MRI was performed on a SUN workstation using a software package (Dr. View; Asahi Kasei Joho System, Tokyo, Japan) using a method described by Kapouleas et al. (*19*).

The net influx constant (Ki) was calculated on a pixel-by-pixel basis using dynamic data with graphical analysis (*20,21*). Regions of interest (ROIs) were placed over the tumor and the ipsilateral cerebellum, using the MR image as an anatomic reference. ROI size of the tumor was approximately 0.64 cm^3 (8.6 × 8.6 × 8.6 mm, 71 pixels), and average Ki values were determined for the area of maximal activity within the tumor. ROI size of the ipsilateral cerebellum was approximately 5.07 cm^3 (17.2 × 17.2 × 17.2 mm, 299 pixels). The Ki ratio of tumor to ipsilateral cerebellum was calculated. The percentage change in the Ki ratio was used to assess the acute effect of radiosurgery on glucose metabolism. Furthermore, to evaluate the late effect of radiosurgery, the percentage decrement in the tumor volume at 5–6 mo after treatment was observed on serial MR or CT images. One patient (patient 6 in Table 1) died 3 wk after the radiosurgery and was excluded from this analysis. Hence, late therapeutic effect was evaluated in 18 irradiated tumors (16 metastatic and 2 primary). Because most of the tumors were round in shape on transaxial and coronal sections, we assumed they were spheres. To calculate the volume, the maximum diameter of the tumor was measured on the contrast-enhanced CT or MR images. The volumes of 2 irregularly shaped tumors of patients 1 and 8 were calculated as combinations of spheres.

RESULTS

Table 2 shows the Ki ratios before and after treatment. Eighteen of the 19 irradiated tumors (17 metastatic and 1 primary meningioma) showed an increase in the Ki ratio (29.7% ± 14.0% [mean ± SD]) compared with nonirradi-

TABLE 2
Net Influx Constant (Ki) (min^{-1}) of Each Tumor Before and After Radiosurgery

Patient no.	Treatment	Pretreatment Ki		Post-treatment		% change in Ki ratio
		Tumor	Cerebellum	Tumor	Cerebellum	
Metastatic						
1	R	0.0357	0.0373	0.0381	0.0286	39.4
	R	0.0258	0.0373	0.0274	0.0286	38.9
2	R*	0.0256	0.0214	0.0424	0.0241	47.2
	R*	0.0246	0.0214	0.0380	0.0241	37.1
	NR	0.0232	0.0214	0.0266	0.0241	2.2
	NR	0.0210	0.0214	0.0253	0.0241	7.0
	R†	0.0171	0.0209	0.0259	0.0200	58.2
	R†	0.0115	0.0209	0.0128	0.0200	16.4
	NR	0.0286	0.0209	0.0292	0.0200	6.6
3	R	0.0212	0.0279	0.0228	0.0213	40.9
	R	0.0182	0.0279	0.0192	0.0213	37.6
4	R*	0.0236	0.0159	0.0179	0.0105	15.4
	R*	0.0646	0.0159	0.0493	0.0105	16.1
	R*	0.0143	0.0159	0.0111	0.0105	17.8
	NR	0.0181	0.0159	0.0126	0.0105	6.2
	NR	0.0262	0.0159	0.0174	0.0105	1.0
5	R*	0.0418	0.0217	0.0340	0.0170	22.3
	R*	0.0511	0.0217	0.0516	0.0170	29.3
	NR	0.0683	0.0217	0.0584	0.0170	9.3
	NR	0.0361	0.0217	0.0283	0.0170	−0.1
	NR	0.0361	0.0217	0.0284	0.0170	0.7
	R†	0.0512	0.0167	0.0559	0.0150	21.3
	R†	0.0268	0.0167	0.0295	0.0150	22.8
	R†	0.0303	0.0167	0.0352	0.0150	29.3
6	R	0.0155	0.0140	0.0249	0.0175	28.8
Primary						
7	R	0.0155	0.0219	0.0142	0.0141	42.6
8	R	0.0323	0.0313	0.0366	0.0347	1.9‡

*First radiosurgery.
†Second radiosurgery.
‡Central neurocytoma (see text for details).
R = radiated; NR = not radiated.

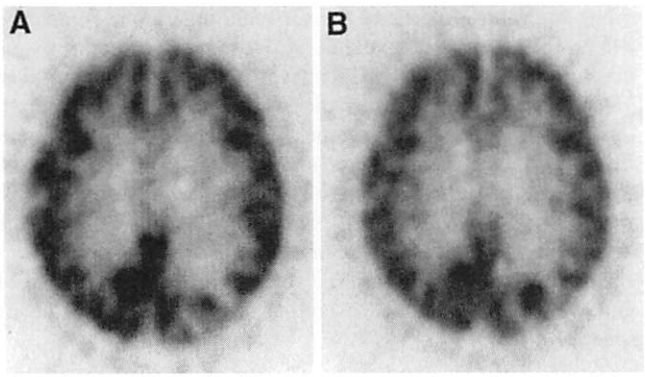

FIGURE 2. Pretreatment (A) and 4 h post-treatment (B) FDG PET images of patient with lung carcinoma (patient 1 in Table 1). Tissue activity images are shown. FDG accumulation of metastatic tumor in left parieto-occipital region, relative to that of gray matter, increased immediately after radiosurgery.

ated tumors (4.1% ± 3.6%, n = 8); this difference was significant ($P < 0.0001$, analysis of variance). The percentage change in the Ki ratio of these 18 tumors ranged from 15.4% to 58.2%. Figure 2 shows an immediate increase in FDG uptake of an irradiated metastatic tumor 4 h after radiosurgery. The central neurocytoma did not show any significant change in Ki ratio (1.9%).

Radiosurgery had a therapeutic effect on most metastatic tumors, demonstrated by a decrease in tumor size on MR or CT images (Fig. 3). Tumors that responded better to the radiosurgery had greater increases in Ki ratio than tumors that responded poorly (Table 3). In 16 irradiated metastatic tumors, percentage volume decrement and percentage increase in the Ki ratio showed a positive correlation ($r = 0.611$, $y = 1.516x - 12.383$, $P = 0.0119$) (Fig. 4). Pretreatment tumor volume was not significantly associated with percentage increase in the Ki ratio ($r = 0.42$, $P = 0.10$). Patient 5, who had 5 metastatic brain tumors from an ocular melanoma, first was treated for 2 tumors and later was treated for the other 3 tumors. Percentage change in the Ki ratio obtained 4 h after the first treatment was 22.3% and 29.3% (Table 2 and Fig. 5). The Ki ratio of the irradiated tumors was 21.8% higher than that of the nonirradiated masses. One nontarget tumor, which was located close (3 cm) to the target tumor and received a dose of 3–5 Gy, showed a slight increase in the Ki ratio (9.3%, Table 2 and Fig. 5). Follow-up FDG PET 2 wk after the first treatment showed that the Ki ratios of the irradiated tumors had fallen below the baseline value (Fig. 5). Follow-up CT confirmed the effectiveness of the radiosurgery by showing a decrease in tumor size (Table 3).

The central neurocytoma showed moderate FDG uptake before treatment, but there was no significant increase after radiosurgery and no change in size after 6 mo (Table 2). The meningioma showed low FDG uptake before treatment and

TABLE 3
Changes in Tumor Volume and Net Influx Constant (Ki)

Patient no.	Volume (cm^3)		% decrease	% change in Ki ratio
	Pretreatment	Post-treatment		
1	1.77	1.15	34.90	39.42
	4.19	2.80	33.01	38.90
2	2.35*	0.45	80.91	47.24
	1.44	0.22	84.63	37.08
	7.23†	3.31	54.20	58.18
	3.05	2.14	29.77	16.38
3	4.51	3.31	26.51	40.86
	1.15	0.70	39.42	37.64
4	4.19*	4.19	0.00	15.44
	0.52	0.45	14.26	16.11
	0.27	0.38	−42.38	17.80
5	5.20*	3.31	36.29	22.34
	1.95*	0.52	73.15	29.32
	1.15†	0.90	21.35	21.63
	2.80†	2.35	16.18	22.82
	2.80†	1.60	43.12	29.29

*First radiosurgery.
†Second radiosurgery.

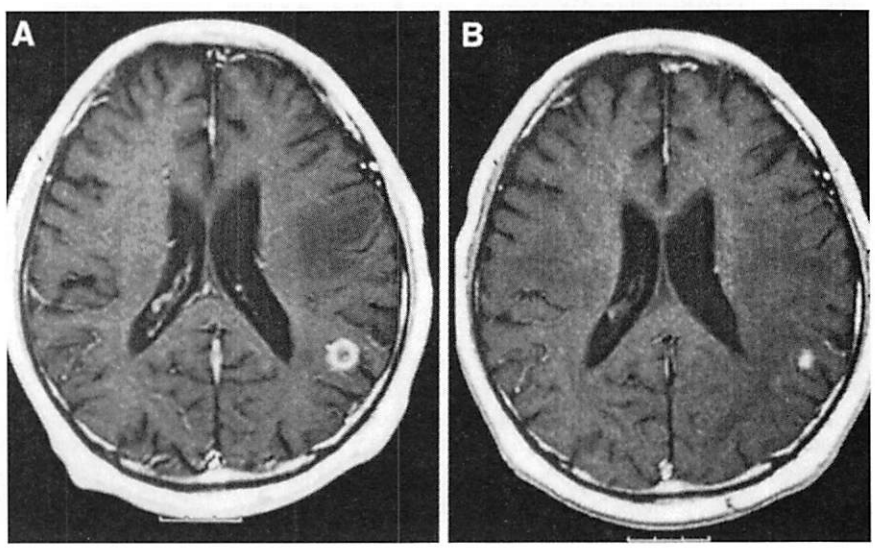

FIGURE 3. Contrast-enhanced MR images of patient with metastatic lung carcinoma before (A) and 6 mo after (B) stereotactic radiosurgery (patient 2 in Table 1). Significant decrease in tumor size confirmed effectiveness of radiosurgery.

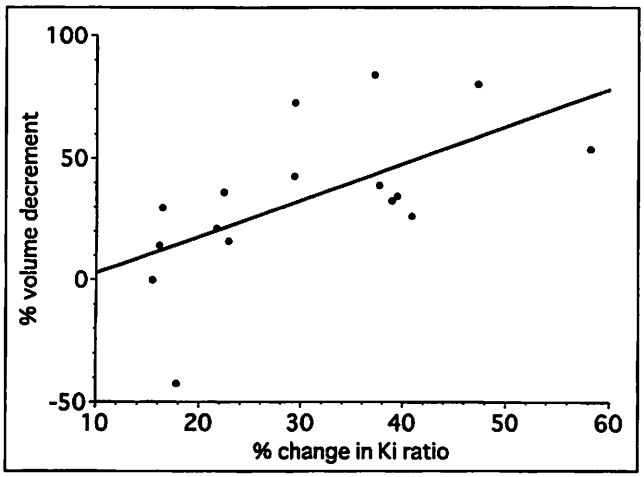

FIGURE 4. Correlation between tumor volume and Ki ratio. There was positive correlation between percentage volume decrement and percentage change in Ki ratio (r = 0.61, y = 1.52x − 12.38).

an apparent increase after radiosurgery. At 6-mo follow-up, there was no decrease in tumor size. Because the response of meningioma to radiotherapy is known to be slow (*22*), the treatment effect may not be well evaluated in this short follow-up period of 6 mo.

DISCUSSION

In this study, we used the Ki of FDG uptake as an index of glucose metabolism of tumors. Ki was the most reliable method for quantification of FDG uptake by the tumors (*23*). The required assumptions are negligible glucose-6-phosphatase activity (k4) and equilibration between tissue and plasma. Ki of lung tumors is independent of uptake period

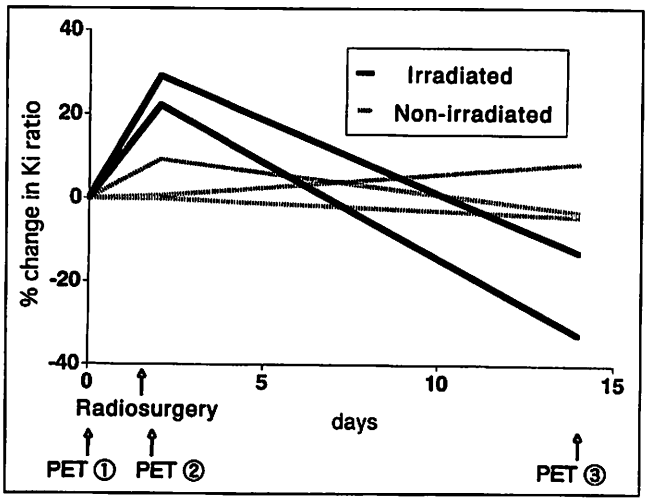

FIGURE 5. Serial changes in Ki ratio of irradiated and nonirradiated tumors relative to pretreatment condition (patient 5). Rapid increase in Ki ratio of irradiated tumors measured 4 h after radiosurgery is shown (solid lines). Follow-up PET scan obtained on day 14 showed decrease in Ki ratio of irradiated tumors below baseline, whereas nonirradiated tumor showed no significant change (dotted lines).

(*24*). To minimize possible confounding effects, such as sedation and plasma glucose level, on the glucose metabolism of the tumors, percentage change in the Ki ratio (tumor-to-cerebellum ratio) was adopted to evaluate glucose metabolism before and after radiosurgery. Because k4 is negligible in brain tissue (*25*), Patlak graphical analysis was properly applied to the brain. Patlak graphical analysis applied to earlier time intervals (10–30 min after FDG injection) causes overestimation of Ki of brain tissue compared with the interval between 50 and 120 min (*25*), probably due to nonequilibration between plasma and brain tissue. The overestimation of Ki of brain tissue, however, is a systematic effect dependent on tissue components (gray matter or white matter) and time interval used for the analysis (*25*). Because relatively large ROIs were placed over the cerebellum and the time interval was kept constant across all studies, Ki of the cerebellum can be used safely to normalize the confounding effect. Hence, percentage change in the Ki ratio of tumors should be understood as being relative to nonirradiated normal brain tissue. This approach is justified in the presence of both irradiated and nonirradiated tumors coexisting simultaneously in the same patient. Because the Ki ratio of irradiated tumors was significantly higher than that of nonirradiated tumors in the same patients, the percentage increase in the Ki ratio represents the acute radiation effect of glucose metabolism of the tumors.

This in vivo study is concordant with a previous in vitro study (*11*), which confirms that the metabolic changes in neoplastic tissues occur as early as 4 h after high-dose irradiation. The mechanisms of the hyperacute increase in glucose metabolism of the irradiated neoplasms are not known. The in vitro studies using baby hamster kidney cells (*26*) showed that cellular stresses such as hyperthermia, chemical substances, infection and treatment of insulin cause the glucose transporter to move from an intracellular site in the perinuclear region to the plasma membrane. The degree of translocation is parallel to the glucose uptake. Widnell et al. (*26*) speculated that cellular stress increases glucose transport by promoting the accumulation of glucose transporter molecules at the cell surface (*26,27*). Hence, increases in glucose uptake may be caused by simple stress responses common to normal cells. However, this study showed that tumors that responded well to the treatment showed a hyperacute increase in FDG uptake that was parallel to the degree of the response, whereas nonresponders did not show any hyperacute change. Therefore, the hyperacute increase in FDG uptake may represent a tumor-specific response to the radiotherapy. It might be speculated that tumor cells require more glycolytic metabolism for energy-consuming processes such as deoxyribonucleic acid (DNA) repair and apoptosis. Through the stabilization of p53 protein, DNA damage leads to programmed cell death (apoptosis) and to G1 arrest to inhibit the replication of damaged DNA, permitting time for repair (*28–31*). Chemotherapies with complex multidrug regimens cause an acute increase in glucose metabolism (*32,33*).

Hence, hyperacute elevation of glucose metabolism may represent an acute rescue system in tumor cells, an energy-consuming process that may be evoked commonly by noxious intervention such as irradiation or chemotherapy. Histological cell type and grade of malignancy may influence this metabolic change, because radiation-induced apoptosis is highly cell-type-dependent (*31*) and may be related to the elevation of glucose metabolism (*9*). In three human tumor xenografts, the most radiosensitive tumor with the highest incidence of radiation-induced apoptosis displayed a 2.3-fold higher rate of FDG accumulation 2 h after irradiation compared with a nonirradiated group, and FDG uptake in the others did not increase significantly (*9*). These findings may explain why the central neurocytoma failed to show a significant increase in FDG uptake after radiosurgery or any late treatment effect.

CONCLUSION

We confirmed that tumor uptake of FDG increased 4 h after stereotactic radiosurgery. FDG PET appears to be a potential tool for evaluating early therapeutic effects of radiosurgery, before morphological changes can be detected by MRI or other imaging modalities. Radiation oncologists may find that serial FDG PET is useful for predicting the outcome of radiosurgery on neoplasms by detecting hyperacute changes in glucose metabolism.

ACKNOWLEDGMENTS

The authors thank Katsuya Sugimoto for PET operation and the staff members of the Biomedical Imaging Research Center, Fukui Medical University. This study was supported in part by research grant JSPS-RFTF97L00203 for the Research for the Future program from the Japan Society for the Promotion of Science.

REFERENCES

1. Warburg O. *The Metabolism of Tumors.* London, UK: Constable & Co.; 1930:254–270.
2. Warburg O. On the origin of cancer cells. *Science.* 1956;123:309–314.
3. Hawkins RA, Choi Y, Huang SC, Messa C, Hoh CK, Phelps ME. Quantitating tumor glucose metabolism with FDG and PET. *J Nucl Med.* 1992;33:339–344.
4. Hawkins RA, Hoh C, Dahlbom M, et al. PET cancer evaluations with FDG. *J Nucl Med.* 1991;32:1555–1558.
5. Coleman RE, Hoffman JM, Hanson MW, Sostman HD, Schold SC. Clinical application of PET for the evaluation of brain tumors. *J Nucl Med.* 1991;32:616–622.
6. Daemen BJ, Elsinga PH, Paans AM, Wieringa AR, Konings AW, Vaalburg W. Radiation-induced inhibition of tumor growth as monitored by PET using L-[1-^{11}C]tyrosine and fluorine-18-fluorodeoxyglucose. *J Nucl Med.* 1992;33:373–379.
7. Bassa P, Kim EE, Inoue T, et al. Evaluation of preoperative chemotherapy using PET with fluorine-18-fluorodeoxyglucose in breast cancer. *J Nucl Med.* 1996;37:931–938.
8. Hautzel H, Muller-Garter H-W. Early changes in fluorine-18-FDG uptake during radiotherapy. *J Nucl Med.* 1997;38:1384–1386.
9. Furuta M, Hasegawa M, Hayakawa K, et al. Rapid rise in FDG uptake in an irradiated human tumour xenograft. *Eur J Nucl Med.* 1997;24:435–438.
10. Rozental JM, Levine RL, Mehta MP, et al. Early changes in tumor metabolism after treatment: the effects of stereotactic radiotherapy. *Int J Radiat Oncol Biol Phys.* 1991;20:1053–1060.
11. Fujibayashi Y, Waki A, Sakahara H, et al. Transient increase in glycolytic metabolism in cultured tumor cells immediately after exposure to ionizing radiation: from gene expression to deoxyglucose uptake. *Radiat Res.* 1997;147:729–734.
12. Datta R, Weichselbaum R, Kufe DW. Ionizing radiation down-regulates histone H1 gene expression by transcriptional and post-transcriptional mechanisms. *Radiat Res.* 1993;133:176–181.
13. Boothman DA, Majmudar G, Johnson T. Immediate x-ray-inducible responses from mammalian cells. *Radiat Res.* 1994;138 (suppl 1):S44–S46.
14. Hartmann GH, Schlegel W, Sturm V, et al. Cerebral radiation surgery using moving field irradiation at a linear accelerator facility. *Int J Radiat Oncol Biol Phys.* 1985;11:1185–1192.
15. Lutz W, Winston KR, Maleki N. A system for stereotactic radiosurgery with a linear accelerator. *Int J Radiat Oncol Biol Phys.* 1988;14:373–381.
16. Takayama M, Nakamura M, Ikezaki H, et al. Stereotactic radiosurgery using a linear accelerator (LINAC): simulation and positioning. *No Shinkei Geka.* 1995;23:223–228.
17. Hamacher K, Coenen HH, Stocklin G. Efficient stereospecific synthesis of no-carrier-added 2-[^{18}F]-fluoro-2-deoxy-D-glucose using aminopolyether supported nucleophilic substitution. *J Nucl Med.* 1986;27:235–238.
18. DeGrado TR, Turkington TG, Williams JJ, Stearns CW, Hoffman JM, Coleman RE. Performance characteristics of a whole-body PET scanner. *J Nucl Med.* 1994;35:1398–1406.
19. Kapouleas I, Alavi A, Alves WM, Gur RE, Weiss DW. Registration of three-dimensional MR and PET images of the human brain without markers. *Radiology.* 1991;181:731–739.
20. Patlak CS, Blasberg RG, Fenstermacher JD. Graphical evaluation of blood-to-brain transfer constants from multiple-time uptake data. *J Cereb Blood Flow Metab.* 1983;3:1–7.
21. Patlak CS, Blasberg RG. Graphical evaluation of blood-to-brain transfer constants from multiple-time uptake data: generalizations. *J Cereb Blood Flow Metab.* 1985;5:584–590.
22. Kida Y, Kobayashi T, Tanaka T, Oyama H, Iwakoshi T. Stereotactic radiosurgery of intracranial meningiomas. *No Shinkei Geka.* 1994;22:621–626.
23. Sadato N, Tsuchida T, Nakamura N, et al. Noninvasive estimation of the net influx constant using standardized uptake value for quantification of FDG uptake of tumors. *Eur J Nucl Med.* 1998,25:559–564.
24. Zasadny KR, Kison PV, Neuhoff A, Wahl RL. Comparison of the influx-constant for FDG as determined from 30-minute and 60-minute dynamic PET scans in patients with lung cancer [abstract]. *J Nucl Med.* 1997;38:244P.
25. Lucignani G, Schmidt KC, Moresco RM, et al. Measurement of regional cerebral glucose utilization with fluorine-18-FDG and PET in heterogeneous tissues: theoretical considerations and practical procedure. *J Nucl Med.* 1993;34:360–369.
26. Widnell CC, Baldwin SA, Davies A, Martin S, Pasternak CA. Cellular stress induces a redistribution of the glucose transporter. *FASEB J.* 1990;4:1634–1637.
27. Sviderskaya EV, Jazrawi E, Baldwin SA, Widnell CC, Pasternak CA. Cellular stress causes accumulation of the glucose transporter at the surface of cells independently on their insulin sensitivity. *J Membr Biol.* 1996;149:133–140.
28. Kastan MB, Onyekwere O, Sidransky D, Vogelstein B, Craig RW. Participation of p53 protein in the cellular response to DNA damage. *Cancer Res.* 1991;51:6304–6311.
29. Hickman JA. Apoptosis as a therapeutic target. In: Yarnold JR, Stratton M, McMillan TJ, eds. *Molecular Biology for Oncologists.* 2nd ed. London, UK: Chapman & Hall; 1996:230–239.
30. Lowe SW, Schmitt EM, Smith SW, Osborne BA, Jacks T. p53 is required for radiation-induced apoptosis in mouse thymocytes. *Nature.* 1993;362:847–849.
31. Clarke AR, Purdie CA, Harrison DJ, et al. Thymocyte apoptosis induced by p53-dependent and independent pathways. *Nature.* 1993;362:849–852.
32. Rozental JM, Cohen JD, Mehta MP, Levine RL, Hanson JM, Nickles RJ. Acute changes in glucose uptake after treatment: the effects of carmustine (BCNU) on human glioblastoma multiforme. *J Neurooncol.* 1993;15:57–66.
33. Haberkorn U, Morr I, Oberdorfer F, et al. Fluorodeoxyglucose uptake in vitro: aspects of method and effects of treatment with gemcitabine. *J Nucl Med.* 1994;35:1842–1850.